Nuclear Engineering PhD Qualifying Exam Part II

A discussion of the paper by Xiaogang Han and Robin P. Gardner in Nuclear Science and Engineering 155 (2007): 'CEARCPG: A Monte Carlo Simulation code for Normal and Coincidence Prompt-Gamma-Ray Neutron Activation Analysis'

North Carolina State University
Raleigh, North Carolina
January 12, 2018

Vincent A. DiNova

Presented to the Q-Committee:

Dr. Dmitriy Anistratov	Dr. David Kropaczek	Dr. Steven Shannon

With Q-Committee chair:

Dr. Robin P. Gardner

1. Motivation

The primary motivation for the development of the CEARCPG coding package was to advance concepts presented by Metwally, Gardner, and Han in the early 2000's. In "A Feasibility Study of a Coincidence Counting Approach for Prompt Gamma Neutron Activation Analysis (PGNAA) Applications (Gardner et al., 2000)" preliminary concepts using coincidence techniques utilizing PGNAA were developed and tested using experiments conducted with the PULSTAR nuclear reactor at NC State University. Several successive papers were written to discuss the simulation, analysis, and design tools needed to develop a comprehensive tool for use in PGNAA applications. This paper will further explore these concepts, previous works, and ultimately the completion of CEARCPG and its consequences on the field.

2. Introduction to PGNAA

Prompt gamma-ray neutron activation analysis is a nondestructive, near real time technique used for bulk material identifications. PGNAA relies on neutron inelastic scatter and capture reactions to produce characteristic gamma-rays used to identify minute amounts of elements in a bulk sample. Due to low cross sections for these reactions, background sources from natural radiation, activation of the NaI detector, and gamma-rays from the decay of the neutron source a low signal to noise ratio (SNR) is common. As such, in order to increase the SNR, a coincidence counting technique is applied.

2.1. Neutron Inelastic Scatter

Neutron inelastic scatter involves an incoming neutron colliding with a target nucleus and exiting with less energy and at a different angle than it entered. The energy deposited on the target nucleus causes it to reach an excited state and rapidly releases a gamma-ray to return to its normal energy state represented in equation 1 as follows:

$$ {}_0^1n + {}_Z^AX \rightarrow {}_0^1n' + {}_Z^AX^* \quad (1) $$

2.2 Neutron Capture

Neutron capture, also denoted as (n, γ), can occur over a wide range of energies and has the highest probability at thermal energies for the elements of interst. The (n, γ) reaction begins when a neutron interacts with a target nucleus and is absorbed. The newly formed nucleus is placed in an excited state, and in order to form a new ground state, at least one γ photon is emitted as shown in eq. 2 below.

$$ {}_0^1n + {}_Z^AX \rightarrow {}_Z^{A+1}X^* \quad (2) $$

Each nucleus (apart from Helium-4) gives off a distinct signature of intensities and energies, allowing for the identification of the sample from the γ photon emissions.

3. CEARPGA I

The first iteration of what became CEARCPG involved a specific Monte Carlo code named CEARPGA I (Shyu et al., 1993). CEARPGA I was developed to analyze bulk materials using the Monte Carlo Linear Least Squares method. Utilizing a 2 μg ^{252}Cf neutron source and 39% HPGe semiconductor detector,

PGNAA spectra were collected thru experimentation. The specific purpose CEARPGA I code then attempted to simulate the same experimental results. The most important aspect of CEARPGA I is the many variance reduction techniques employed to minimize the computation time to run each simulation. The next section will explore how the variance reduction techniques are employed.

3.1 CEARPGA Variance Reduction Techniques

3.1.1 Russian Roulette

Used in conjunction with the expected value technique, Russian Roulette randomly terminates either a neutron history or photon-tracking when the associated weight falls below a preassigned value, w_{min}. Once the particle weight drops below w_{min}, a random number ξ, of value between 0 and 1, compares the weight to the ratio of the particle weight and w_{min}. If $\xi \leq w/w_{min}$, then the particle survives, and the weight will be raised to w_{min}, otherwise the neutron history or photon-tracking is terminated.

3.1.2 Truncated Exponential PDF

A feature to ensure that proper sampling is performed inside each cell of importance, the truncated exponential PDF measures the distance d to interaction and determines if the distance D to the cell boundary lies within the range. If the cell boundary is not within the system boundary, the normal exponential PDF is used to determine the flight distance d:

$$p(x) = \Sigma_t \exp(-\Sigma_t x), for\ 0 \leq x \leq \infty \tag{3}$$

Where Σ_t is the macroscopic total cross section of the cell and the distance d is determined by:

$$d = -\frac{1}{\Sigma_t} \ln \xi \tag{4}$$

If the cell boundary is also the system boundary, the truncated exponential PDF is applied to force an interaction to occur within the system and ensure that neutrons do not escape the boundary. The truncated exponential PDF is described by:

$$p(x) = \frac{\Sigma_t \exp(-\Sigma_t x)}{1 - \exp(-\Sigma_t D)}, for\ 0 \leq x \leq D \tag{5}$$

In this case, the sampled flight distance d is determined by:

$$d = -\frac{1}{\Sigma_t} \ln\{1 - \xi\,[1 - \exp(-\Sigma_t D)]\} \tag{6}$$

Where ξ is a random number between 0 and 1. Note: the neutron weight must also be adjusted due to the biased sampling by multiplying the weight with the adjusting factor given as:

$$w_{adj} = 1 - \exp(-\Sigma_t D) \tag{7}$$

If the distance d ≤ D, the next interaction position will be in the same cell or at the boundary. This indicates that the sampling process of flight distance to the next interaction is complete and the next position is calculated by:

$$\begin{aligned} x &= x_0 + d\Omega_1 \\ y &= y_0 + d\Omega_2 \\ z &= z_0 + d\Omega_3 \end{aligned} \tag{8}$$

Where (x_0, y_0, z_0) is the current position. Conversely, if d ≥ D, the neutron will enter a new cell along the current direction, and the sampling process for the flight distance of the neutron will continue. Here, the neutron will move to the cell boundary at a new position (x, y, z):

$$\begin{aligned} x &= x_0 + D\Omega_1 \\ y &= y_0 + D\Omega_2 \\ z &= z_0 + D\Omega_3 \end{aligned} \tag{9}$$

3.1.3 Direction Biasing

The previous section discussed the methodology of ensuring that a collision occurs within the system boundary, reducing the amount of computation time wasted on particles that would otherwise have exited the system and not contributed to the spectra. A similar technique is used to ensure that once a photon is emitted, each direction is sampled and only those that will intersect the detector are allowed to continue. Before going into the sampling technique for direction biasing, the neutron interactions must be sampled:

Begin by assuming a predefined direction $(\mathrm{u}, \mathrm{v}, \mathrm{w})$ and a true PDF $f(v)$, with μ being the cosine of the angle between this predefined direction and the sampled new direction. Instead of sampling from the true PDF, μ is sampled from a new PDF $g(v)$. By defining $x = 1 - \mu$, the new PDF $g'(x), g'(x) = f(v)$, has the form:

$$g'(x) = a * \mathrm{e}^{-\mathrm{bx}}, for\ 0 \leq x \leq 2 \tag{10}$$

This can further be normalized, yielding $a = \frac{b}{1-\exp(-2b)}$. From this relationship, the sampled random number can be described as:

$$\xi = \int_0^x g'(x')dx', \tag{11}$$

With the sampled μ becoming:

$$\mu = -\frac{1}{b}\ln\left[1-\xi\left(1-\mathrm{e}^{-2\mathrm{b}}\right)\right], \tag{12}$$

And the associated adjusting weight $w_{adj} = \frac{f(\mu)}{f'(\mu)}$. There are different treatments for whether the photons are primary or secondary. Primary photons, those defined as being emitted directly from fission, inelastic scattering, or radiative capture, are given a predefined direction $(\mathrm{u}, \mathrm{v}, \mathrm{w})$ defined as the direction from the present position to the center of the detector. By assuming that these photons are emitted isotropically, the true PDF $f(v)$, in this case, would be $f(v) = \frac{1}{2}$, for $v \in [-1, 1]$. The weight also must be adjusted for this scenario and would become $w_{adj} = \frac{1}{[2f'(\mu)]}$. The secondary photons, produced after a Compton scattering event, are assigned a predefined direction (u, v, w) defined to be the initial photon direction before the scattering event. Note: the previous direction is towards the center of the detector, thus preserving the direction of the secondary photons to the center of the detector as well. The true PDF for the photons having a Compton scattering event can be obtained by normalizing the Klein-Nishina differential scattering cross section (Evans, 1955).

$$\sigma_c(E) = \pi Z r_e^2 \lambda \left[(1-2\lambda-2\lambda^2)\ln\left(1+\frac{2}{\lambda}\right) + \frac{2(1+9\lambda+9\lambda^2+2\lambda^3)}{(\lambda+2)^2}\right] \tag{13}$$

3.1.4 Discrete Importance Function

Importance sampling (Cater and Cashwell, 1975) describes that a discrete PDF can be applied as follows:

Suppose $E_1,\ldots,E_n$ are n independent, mutually exclusive events with corresponding probabilities $p_1,\ldots,p_n$ where $p_1+\ldots+p_n=1$. Define a discrete importance function I_i as the importance of an event E_i. The fictitious discrete PDF then becomes:

$$p'_i = \frac{I_i p_i}{C}, for\ i = 1, \ldots, n \tag{14}$$

Where

$$C = \sum_{i=1}^{n} I_i P_i \tag{15}$$

A random number is generated to determine which event is to occur such that $p'_1 + \cdots + p'_{i-1} \leq \xi < p'_1 + \cdots p'_i$. The corresponding weight adjustment would be $w_{adj} = \frac{p_i}{p'} = \frac{C}{I_i}$. Note: to sample a true PDF, each importance should be set equal, and assigning a value of 0 would place zero importance, or prevent the corresponding event from occurring. The deployment of this technique is discussed below. For a given interaction, assume that the total macroscopic total cross sections for interaction types 1, 2, 3…n be represented a $\Sigma_1, \Sigma_2, \Sigma_3, \ldots \Sigma_n$ respectfully. The probability mass function for interaction type can then be represented as:

$$p_i = \frac{\Sigma_i}{\sum_{j=1}^{n} \Sigma_j}, for\ i = 1, 2, 3, \dots n \tag{16}$$

Explicit sampling is used to force the neutron to undergo elastic scattering or inelastic scattering and radiative capture. This technique increases the number of neutron scattering and capture interactions. At each interaction position discussed in the previous section, the neutron is divided into two parts. One will undergo neutron inelastic scattering or elastic scattering selected by analog sampling. The scattered neutron will continue to each successive interaction site until killed by Russian Roulette detailed in section 3.1.1. The second neutron in this scenario is forced to undergo radiative capture, and a weighting factor is used to keep track of any changes. Using Σ_{inel}, Σ_{el}, and Σ_{cp} to refer to the cross section of neutron inelastic scatter, elastic scatter, and radiative capture, the weighting factor for the first split neutron becomes:

$$W_1 = W_0 \frac{\Sigma_{inel} + \Sigma_{el}}{\Sigma_{TOT}} \tag{17}$$

Where W_0 is the original weight of the neutron and Σ_{TOT} is the total macroscopic cross section. Similarly, for the second neutron, the weight will become:

$$W_1 = W_0 \frac{\Sigma_{cp}}{\Sigma_{TOT}} \tag{18}$$

Finally, the interaction type is sampled between the neutron inelastic scattering reaction and the elastic scattering reaction. A random number ξ between 0 and 1 is sampled. Neutron inelastic scattering will be sampled if $\xi \leq \frac{\Sigma_{inel}}{\Sigma_{inel+}\Sigma_{el}}$, otherwise the elastic scattering reaction is sampled.

3.1.5 Unscattered Detection Probability Estimator/Expected Value Technique

The expected value of the unscattered detection probability of a photon, emitted from fission, inelastic scattering, or radiative capture or scattered from Compton scattering is:

$$P = \int_{v_{min}}^{v_{max}} \int_{p_{min}(v)}^{p_{max}(v)} p_1(v,p) \cdot p_2(v,p) \cdot p_3(v,p) dp dv \tag{19}$$

Where

$p_1(v,p)$ = the probability of scattering or emitting toward the detector through angles (v,p)

$$p_2(v,p) = \exp\left[-\sum_{i=1}^{n} \mu_i l_i(v,p)\right]$$

= the probability that the photon will be transmitted to the detector with the direction angles (v,p) without collision, with μ_i and l_i being the linear attenuation coefficient of zone I and path length through zone i respectively.

$p_3(v,p) = 1 - exp[-\mu_D l_D(v,p)]$

=the detection probability with μ_D and $l_D$being the linear attenuation coefficient and path length in the detector respectively.

3.2 General Characteristic of CEARPGA I

The neutron interactions considered in CEARPGA I are elastic scattering, radiative capture, and inelastic scattering using the ENDF/B-V cross section data. The cross section for hydrogen is separate, due to the influence of the reduced mass effect. CEARPGA incorporates the cross sections from an experiment from Beyster et al. (1965) to compensate for the bound hydrogen. Photon cross sections are based on a compilation of Storm and Israel (1967).

4. CEARPGA II

The CEARPGA I code successfully demonstrated the ability to create spectra to be used in MCLLS analysis of coal; however, some improvements needed to be made. The primary concern identified was the "big weight" problem that distorted the lower energy regions of the spectra. The problem was identified by Gardner (2000) as deriving from the expected value splitting approach detailed in section 3.1.5. From eq. 18, an issue can be surmised that γ photons generated near the detector have large angles subtended by the detector, short flight distances, and large probabilities for reaching the detector without interaction.

Additional issues that were discovered include the nonlinear response of detectors not being included in the original coding package, the inability to generate background libraries for NaI activation or natural background, and the 0.511-MeV annihilation γ photons generated from pair production outside the detector were not tracked due to the minimum cutoff energy being set at 1 MeV.

CEARPGA II continued to use major elements of CEARPGA I including:

1) Use of stratified sampling to force all γ rays to be emitted from the source, as well as the capture and inelastic neutron interactions
2) Use of detector response functions to generate pulse-height libraries
3) Use of correlated sampling to predict small changes in composition
4) Forcing neutron interactions prior to the system boundary to prevent lost events

The next sections describe in detail the improvements that were made in CEARPGA II.

4.1 Generation of NaI Detector Response Functions

A specific-purpose Monte Carlo simulation code, G03, was incorporated into CEARPGA II. G03 generates detector response functions for NaI detectors, which are spread according to a Gaussian distribution described by:

$$\sigma_N(E_I) = \sqrt{\left[\sigma_T^2(E_{I)} - \sigma_I^2(E_I)\right]} \tag{20}$$

And

$$\sigma_T(E_I) = aE_I^b \tag{21}$$

Where $\sigma_T(E_I)$ is the total standard deviation of the NaI detector response for a γ photon of energy E_I, a and b are fitted parameters, and $\sigma_I(E_I)$ is the standard deviation from the NaI detector inherent nonlinearity caused by non-uniform scintillation efficiencies with deposited electron energies inside the detector. Values for a and b are determined through experimentation and should always be calculated for each detector used.

An intrinsic quality of many detectors is the nonlinearity caused by non-uniform scintillation efficiencies in deposited electron energies. In order to account for this effect in NaI detectors, the following relationship was introduced (Valentine et al., 1998):

$$S(E_e) = 1 + k_1 \exp\left[-\frac{(lnE_e - k_2)^2}{k_3}\right], for\ E_e \geq 10$$

and (22)

$$S(E_e) = 1 + k_1 \exp\left[-\frac{(lnE_e - k_2)^2}{k_4}\right], for\ E_e \leq 10$$

Where $S(E_e)$ is the relative NaI scintillation efficiency for a deposited electron energy E_e in keV.

Additional considerations were put into correcting the variable flat continuum problem addressed by Gardner and Sood (2004). The flat continuum problem is thought to be caused by either the loss of electrons that escape from the detector without full energy deposition or by electrons that are produced from capture at impurity sites.

4.2 Analog Linear Interpolation Approach (ALI)

In an effort to correct the "big weight" problem, the Analog Linear Interpolation Approach (ALI) was devised. Combining Analog Monte Carlo Simulation and the linear interpolation technique, ALI is applied specifically to γ ray photons generated by neutron radiative capture, radioisotope decays in the sample region, and the natural background. Once a tracked neutron enters the sample region, and the radiative capture interaction is chosen, only pseudo γ rays are forced to be emitted and are tracked

separately by an analog Monte Carlo approach. The implementation of ALI is described as follows (Zhang, 2005):

A set of pseudo γ photons is selected to represent those generated from neutron radiative capture, radioisotope decay, and natural background. These must span the energy range of the actual γ photon energies so that interpolation can be used instead of extrapolation. 24 pseudo γ photons are used, with energies from 0.5 MeV to 12 MeV in intervals of 0.5 MeV. The initial weight is given by:

$$W = \frac{W_0}{\Sigma_t} \tag{23}$$

Where W_0 is the cumulative weight of the neutron and Σ_t is the total radiative capture cross section of the sample material. To reduce the statistical error, each photon is tracked a number of times independently. Trial and error was used to determine the sampling number, which was determined to be best at around 100 (Zhang and Gardner, 2005). The score of an incident γ photon is a product of the weight accumulated along the track to the detector and the detector efficiency calculated by:

$$\varepsilon = 1 - e^{-(\Sigma_t l)} \tag{24}$$

Where Σ_t is the total cross section of the incident γ ray in the detector and l is the intersection length of the incident γ ray flight path with the detector. All scores are recorded to a set of energy-score tables of two dimensions, one representing the energy expressed in terms of the channel number and the other representing the scores that originate from the same pseudo γ ray of interest. The energy channel N for the incident γ ray of energy E_f is determined by:

$$(N-1)\cdot \Delta E < E_f \leq N \cdot \Delta E \tag{25}$$

Where ΔE is the energy increment between two consecutive channels. For pseudo γ rays that produce a pair production interaction outside the detector, its score cannot be recorded until the tracking of both 0.511 MeV γ rays is finished. Once a set of energy-score tables is generated, linear interpolation is used to derive the incident spectrum for any γ ray generated in the sample region. For M pseudo prompt γ rays with energies ranging from $E_0, \ldots, E_{M-1}$ and energy-scores of $T_0, \ldots, T_{M-1}$ with maximum channel numbers $N_0^{max}, \ldots, N_{M-1}^{max}$, the interpolation procedure can be determined as follows.

For an incident γ ray energy E in the range between E_{k-1} and E_k, where $k \leq M-1$, energy-score tables T_{k-1} and T_k are used for interpolation. As an exception, if E is $\leq E_1$, the first two tables are chosen (T_1 and T_2). The selected energy-score tables are then adjusted such that the scores are redistributed within the same channels whose range is determined by the interpolated γ ray energy. The adjusting procedure for the selected pseudo γ ray energy score is described as follows:

1) Assign the score in the full energy channel N^{max} to the channel N_{in}^{max}.

2) Assign the total scores between channels $\frac{(K-1)(N^{max}-1)}{(N_{in}^{max}-1)}$ and $\frac{K(N^{max}-1)}{(N_{in}^{max}-1)}$ of the selected energy-score table to the channel K of the modified energy-score table $(K = 1, 2, \dots, N_{in}^{max} - 1)$.

The scores of the incident γ rays with unit weight are interpolated by calculating S^i, the interpolated score the energy channel i of the γ ray of concern, by the following equation:

$$S^i = \frac{\left[\left(lnE - lnE_{k-1}\right) \cdot S_K^i + (lnE_k - lnE) \cdot S_{k-1}^i\right]}{lnE_k - lnE_{k-1}} \quad (26)$$

To generate a spectra, the ALI is applied to derive the incident γ rays using the energy-score tables by the following procedure:

1) Select the element of interest.
2) Determine the γ ray energy and its yield that needs to be interpolated.
3) For each γ ray, interpolate the energy-score tables to obtain its corresponding incident spectrum.
4) Modify the incident spectrum by multiplying appropriate adjusting factors.
5) Add the interpolated incident spectrum to the total incident γ ray spectrum of the element of interest.
6) Repeat steps 2 thought 5 until the interpolations for all γ rays associated with the element have been completed.

4.3 General Characteristics of CEARPGA II

The neutron cross sections are identical to those described for CEARPGA I. Photon cross sections were extracted from the ENDF/B-VI Release 8 EPDL library.

5. CEARCPG

CEARCPG is a specific purpose Monte Carlo code, developed at the Center for Engineering Applications of Radioisotopes (CEAR) group at NC State, with the capabilities of simulating coincidence, anti-coincidence, time-of-flight, and standard (non-coincidence) PGNAA simulations. The coincidence sampling scheme can be illustrated by observing the Q-value energy levels of a ^{13}C radioisotope produced through a $^{12}C(n,\gamma)^{13}C$ reaction shown in figure 1. The Q-value for this reaction is 4.946 MeV. The nuclear structure data is found in the ENSDF nuclear library data and the IAEA PGAA nuclear data library. The ENSDF nuclear data has the information for each individual prompt γ ray, including the energy, relative intensity, and structure information. From the decay scheme, the relationship among prompt γ rays is known. The neutron cross sections have been updated to use the ENDF/B-VI 8300K and JENDL-3 3300K libraries, and the γ ray libraries come from EPDL 97 which include elements $Z = 1 - 100$ and range from 0.01 to 20 MeV.

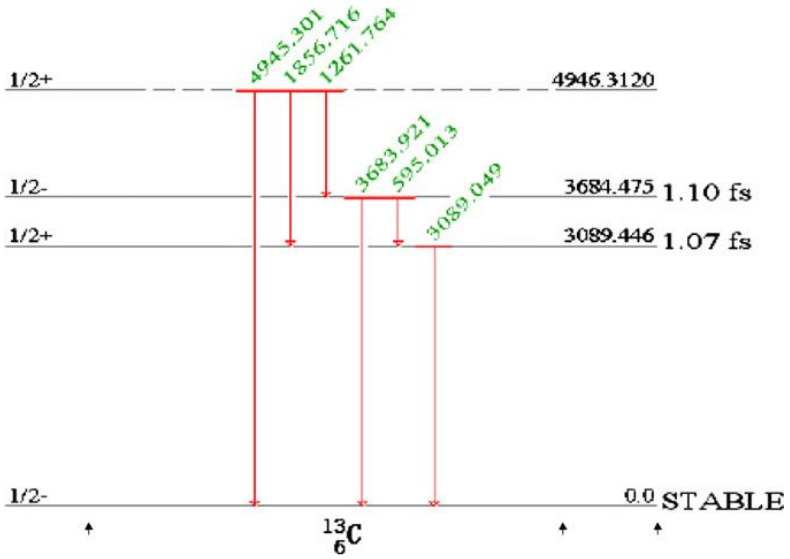

Figure 1. The excitation scheme of C-13. From Han (2007)

Input cards for the geometry are of the same format as MCNP5, allowing for editing software such as VisED to be utilized to view and edit material and cell information. All of the variance reduction techniques from CEARPGA I and II have been included and can be turned on or off by the user in initiation input decks.

6. Benchmark Experiments

Single and coincidence spectra were simulated to analyze three experiments on the Energy Technologies, Inc. (ETI) coal analyzer. These experiments were conducted to determine the levels of Sulfur and Mercury in 6 coal samples by collecting data for 5 hours with a $2.9\ \mu g\ ^{252}Cf$ spontaneous fission neutron source and two 6x6 NaI detectors. Since the ETI coal analyzer only consists of 1 detector, a preliminary test was run to compare CEARCPG and MCNP5. Figure 2 shows the experimental setup for these tests. $2 \cdot 10^5$ histories were generated in CEARPGA and 2 separate MCNP5 runs, one for the neutron source and the other for the γ rays produced by the neutron source, to account for spectra that were then normalized to the nitrogen peak and compared in figure 3.

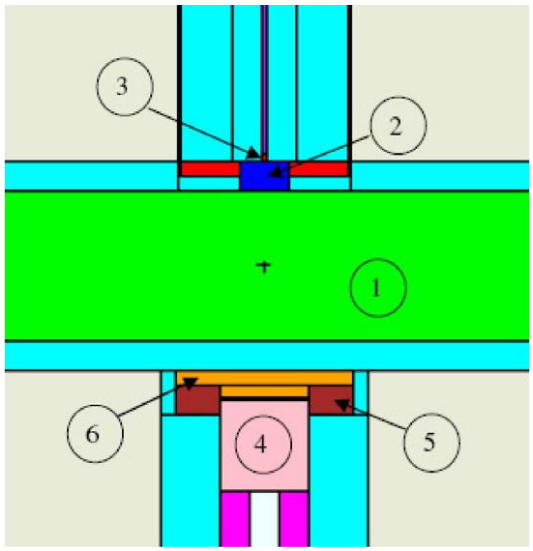

Figure 2. Schematic of the ETI prototype, (1) coal sample, (2) polyethylene, (3) neutron source, (4) NaI detector, (5) shielding, (6) lithium loaded polyethylene. From Han (2007)

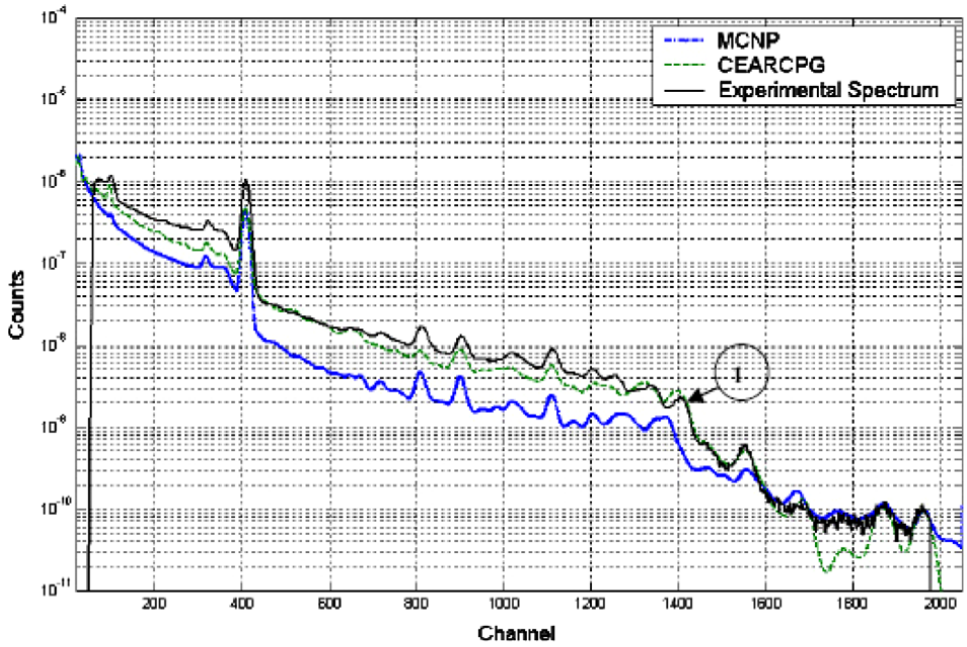

Figure 3. Comparative results between MCNP5 and CEARPGA against the ETI prototype experiments. From Han (2007)

Note: marker 1 on figure 3 illustrates that MCNP does not account for the activation of the NaI peak.

A second experiment was then conducted to introduce the coincidence counting technique. A rectangular coal chute located between the source and the detectors, delivers coal through the detection region for online measurement. Simulations were run for both MCNP5 and CEARCPG and normalized at the hydrogen peak. Fitting to the experimental spectra was not conducted. Figures 4 and 5 below show the experimental setup and resulting spectra.

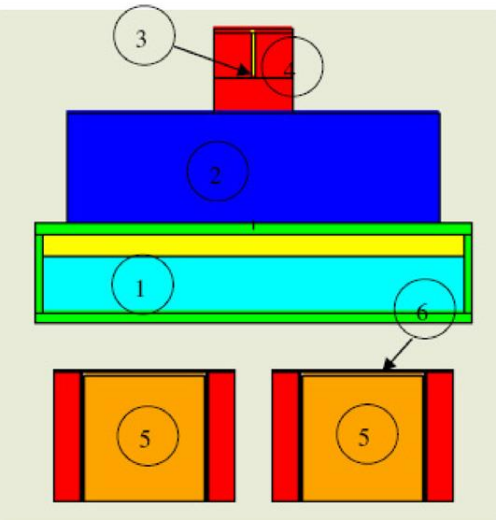

Figure 4. Schematic of the coincidence experiment, (1) coal sample, (2) polyethylene, (3) neutron source, (4) lead shield, (5) NaI detectors, (6) lithium loaded polyethylene. From Han (2007)

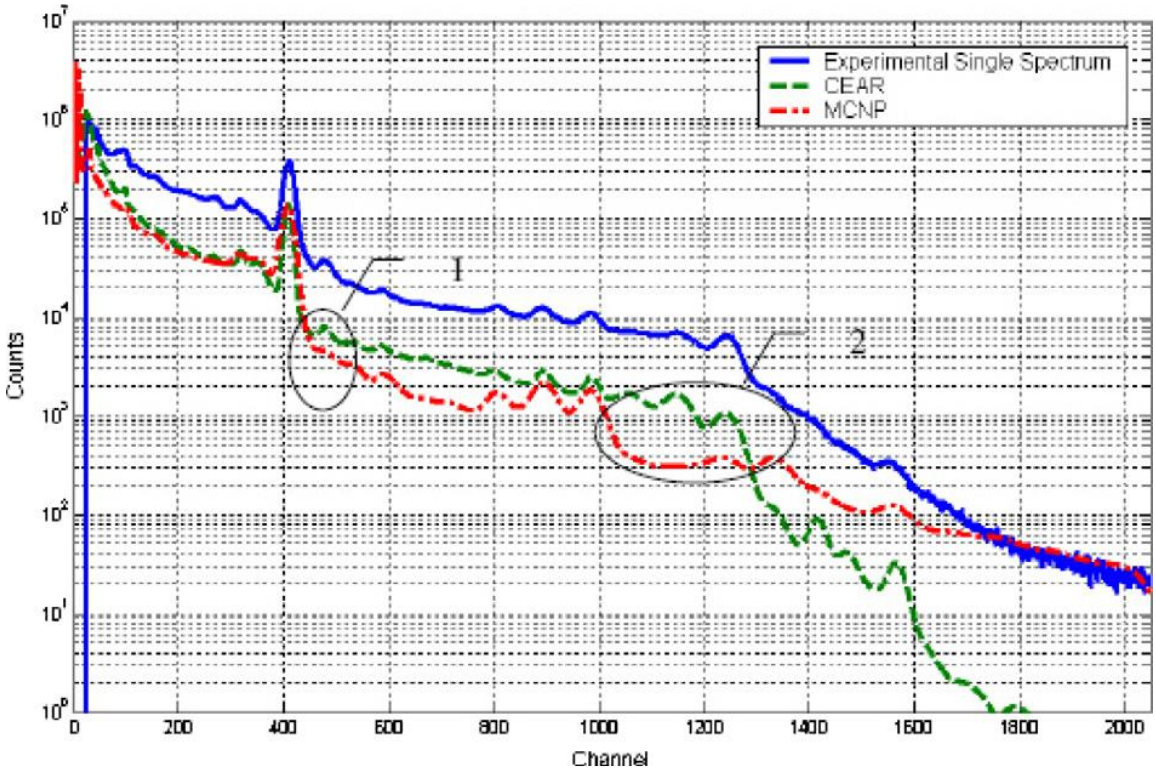

Figure 5. Experimental and simulated singles spectra of the pure sulfur sample. From Han (2007)

Several observations are noticed from these results. First, the spectrum generated by MCNP5 has a greater accuracy in the high-energy region. This is possibly due to better statistics from using a greater number of histories. The other differences in the spectral response is cited as resulting from not accounting for background in this calculation.

The major exclusion in figure 5 is the coincidence measurements that can only be conducted using CEARCPG. Using the SPARROW multiparamater acquisition system, two-dimensional coincidence spectra can be obtained. A diagonal window Q-value summing technique can then be applied to use the two-dimensional spectrum to generate a coincidence spectrum (Hoogenboom, 1958 and Metwally et al., 2005). Figures 6 and 7 below show the two-dimensional Q-value spectra for the sulfur example.

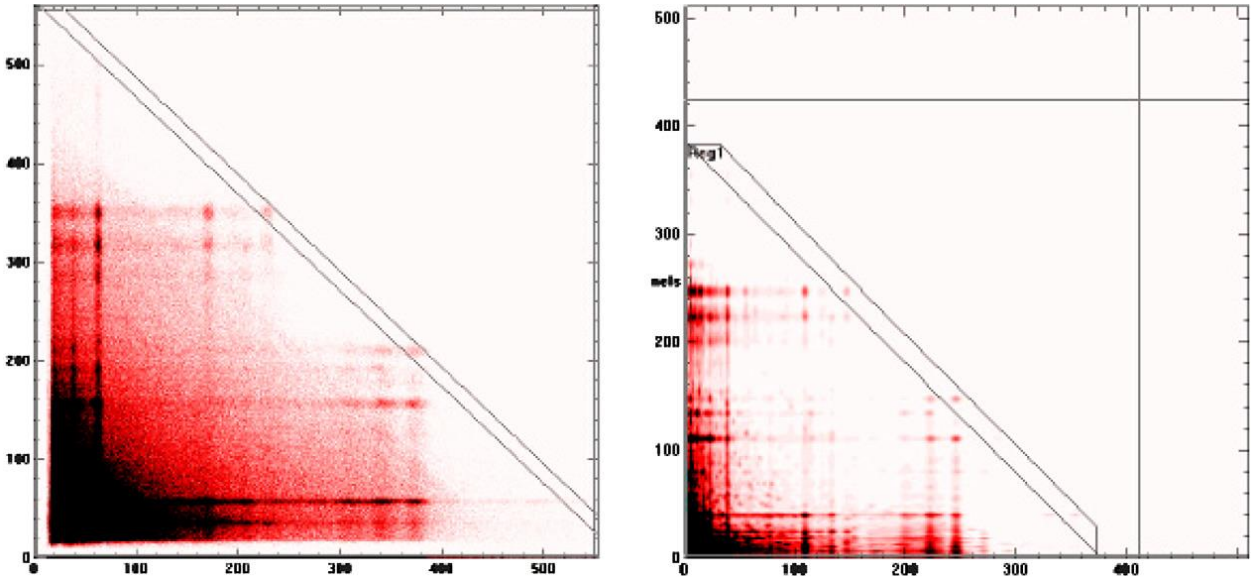

Figure 6. The coincidence spectra of a pure sulfure sample. (a) the experimental coincidence spectrum; (b) the calculated coincidence spectrum. From Han (2007)

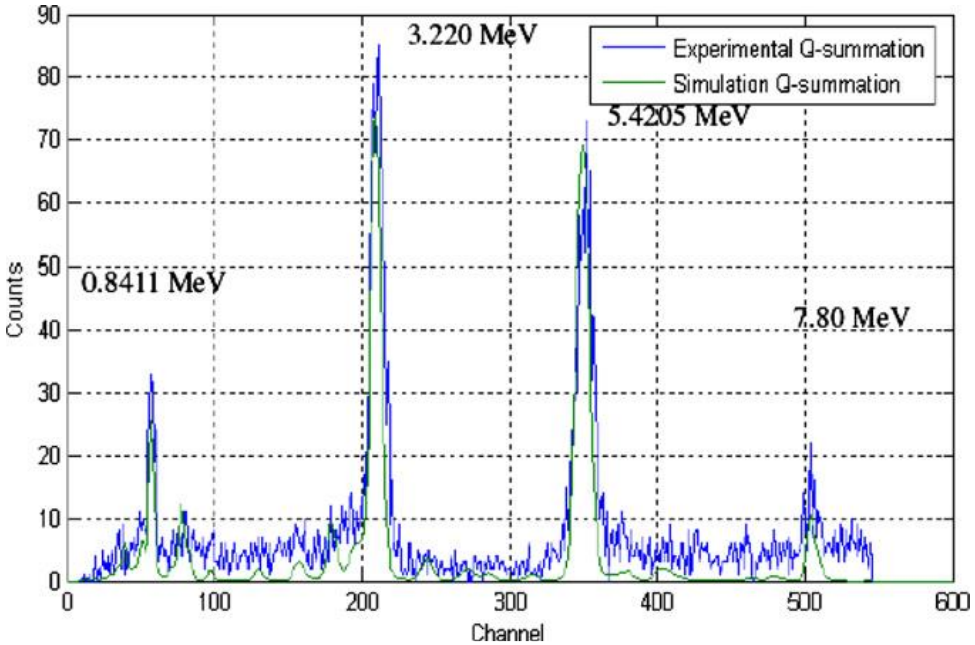

Figure 7. Comparison between the experimental Q-value projection spectrum and the calculated spectrum. From Han (2007)

A final experiment was conducted using the PULSTAR nuclear reactor at NC State University on a pure Mercury sample. Figures 8 and 9 below show the two-dimensional Q-value spectra for the Mercury example.

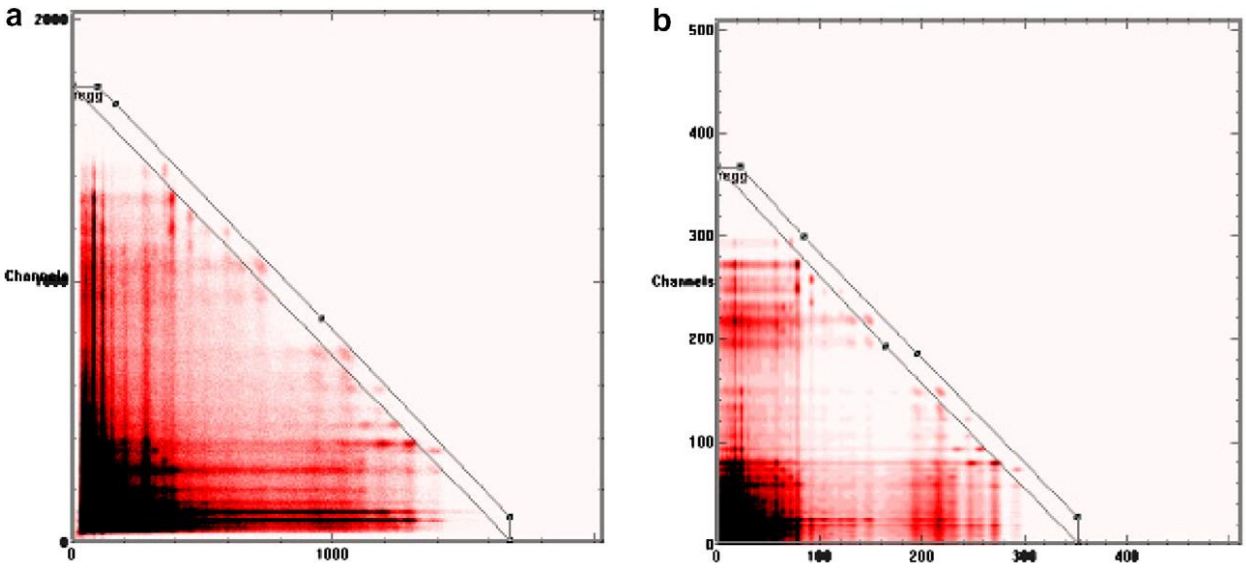

Figure 8. The experimental two-dimensional spectrum versus the calculated two-dimensional spectrum of the Mercury sample. From Han (2007)

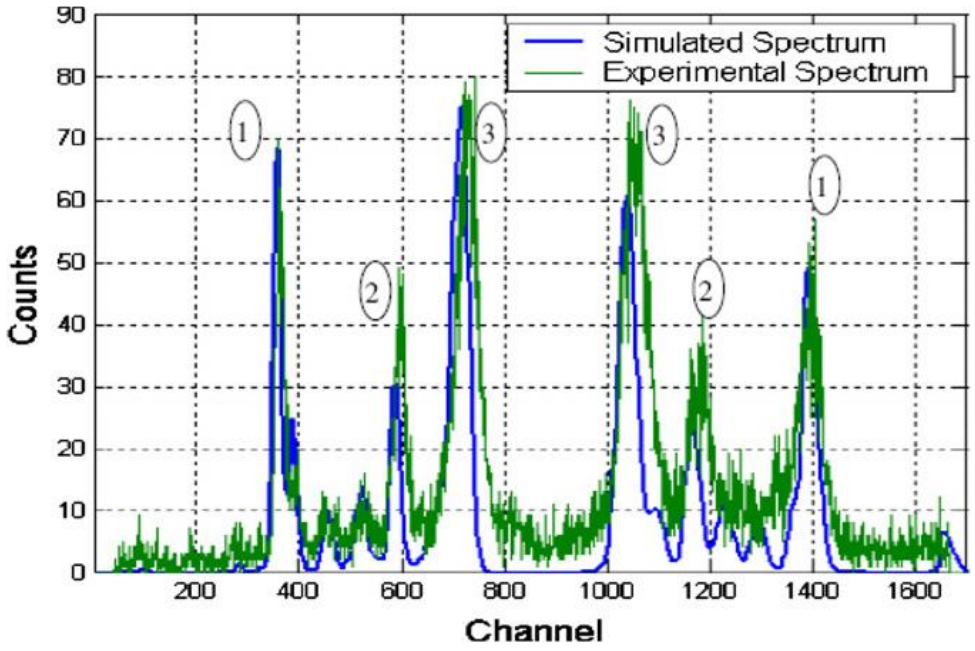

Figure 9. The Q-value projection spectrum of the Mercury sample. From Han (2007)

7. Results

The results of the experiment showed that CEARCPG lowered the reduced Chi-squared over both MCNP5 simulations and CEARCPG I and II calculations. The coincidence technique proved to be a viable method to reduce the impact of background sources and highlight only information relevant to the user.

8. Critique and Discussion

Currently, many types of coal analyzers similar to the one discussed in this paper are being used by the coal industry. The coincidence method, although appearing promising in the results of this investigation, may reduce the signal too much for practical use in situ. Current research is leaning away from the use of ^{252}Cf as a neutron source as it does not occur naturally and is a potential threat to be used in dirty bombs. An alternative approach is emerging by using a DT pulsed generator as a neutron source. There are several advantages that arise from that technology including generating background spectra in between pulses, a smaller range of emitted neutron energies, and eliminating the ability to use the source as a weapon.

Several additional problems were not discussed that could also be overcome with newer technologies. The use of NaI detectors has been commonplace for many decades, but new detectors are becoming available that have qualities that could enhance PGNAA analysis techniques. Due to the vast number of incoming γ ray energies and the low resolution of NaI, many of the peaks do not appear distinct. In order to determine the proper contribution of each γ ray, deconvolution techniques need to be utilized. A new form of semiconductor named CZT could overcome this by offering a much higher resolution. CZT does not have as high of a resolution as HPGe detectors commonly used for applications that require it, but can be used at room temperatures without a loss of resolution or degradation of the material.

Pulse pile up can also introduce complications to PGNAA systems due to the high counting rate. New scintillator detectors such as LaBr and CeBr can help overcome pulse pile up effects with a resolving time > 20 times lower than that of NaI and offering a greater resolution. LaBr does have a downside in that Lanthanum is naturally radioactive and will contribute an additional peak that must be accounted for.

Another advancement being made across many disciplines involves machine learning. Machine learning has the capability of analyzing solutions without the assistance of human backing. Typical operations of coal plants have several workers in a control room monitoring the activities of the plant. Machine learning techniques such as LASSO or Bayesian analysis may offer greater flexibility of the operators by not requiring constant monitoring of the coal feed systems.

9. Bibliography

Bevington, P.R., and Robinson, D.K., "Data Reduction and Error Analysis for the Physical Sciences." McGraw-Hill, Boston (2002).

Carter, L.L., and Cashwell, E.D., "Particle-Transport Simulation with the Monte Carlo Method," TID-26607, U.S. Department of Energy (1975).

Evans, R.D., "The Atomic Nucleus." McGraw-Hill, New York (1955).

Gardner, R. P., et al., "A Feasibility Study of a Coincidence Counting Approach for PGNAA Applications." *Applied Radiation and Isotopes*, 53, (2000).

Gardner, R.P., and Sood, A., "A Monte Carlo Simulation Approach for Generating NaI Detector Response Functions (DRF's) that Accounts for Nonlinearity and Variable Flat Continua," *Nucl. Instrum. Methods B*, 213, 87 (2004).

Han, Xiaogang, and Gardner, R.P., "The Monte Carlo Code CEARCPG for Coincidence Prompt Gamma-Ray Neutron Activation Analysis." *Nuclear Instruments and Methods in Physics Research B*, 263, (2007).

Han, Xiaogang, et al., "CEARCPG: A Monte Carlo Simulation Code for Normal and Coincidence Prompt-Gama-Ray Neutron Activation Analysis." *Nuclear Science and Engineering*, 155, (2007).

Hoogenboom, A.M., "A New Method in Gamma-Ray Spectroscopy: A Two Crystal Scintillation Spectrometer with Improved Resolution," *Nucl. Instrum.*, 3, 57, (1958).

Knoll G., "Radiation Detection and Measurement." Wiley, New York (1989).

Metwally, W.A., et al., "Elemental PGNAA Analysis Using Gamma-Gamma Coincidence Counting with the Library Least-Squares Approach." *Nuclear Instruments and Methods in Physics Research B*, 213, (2004).

Metwally, W.A., et al., "Two-Dimensional Diagonal Summing of Coincidence Spectra for Bulk PGNAA Applications." *Nuclear Instruments and Methods in Physics Research A*, 525, (2004).

Metwally, W.A., et al., "Coincidence Counting for PGNAA Application: Is It the Optimum Method?" J. *Radioanal. Nucl. Chem.,* 265, 2, 309, (2005).

Shyu, C.M., Gardner, R.P., and Verghese, K., "Development of the Monte Carlo – Library Least-Squares Method of Analysis for Neutron Capture Prompt Gamma-Ray Analyzers", *Nuclear Geophysics*, Vol. 7, No. 2, (1993).

Valentine, J.D., Rooney, B.D., and Dorenbros, P., "More on the Scintillation Response of NaI(Tl)," *IEEE Trans. Nucl. SCI.*, 45, 3, 1750 (1998).

Valentine, J.D., Rooney, B.D., and Li, J., "The Light Yield Nonproportionality Component of Scintillator Energy Resolution," *IEEE Trans. Nucl. Sci.*, 45, 3, 512, (1998).

Wang, Jaixin, et al. “Monte Carlo Investigation and Optimization of Coincidence Prompt Gamma-Ray Neutron Activation Analysis.” *Nuclear Instruments and Methods in Physics Research A*, 652, (2011).

Zhang, Wenchao, and Robin P. Gardner. “CEARPGA II: A Monte Carlo Simulation Code for Prompt-Gamma-Ray Neutron Activation Analysis.” *Nuclear Science and Engineering*, 151, (2005).